Polymeric precursor derived nanocrystalline ZnO thin films using EDTA as chelating agent

Uma Choppali [a*1], *Elias Kougianos*[b], *Saraju P. Mohanty*[b], *and Brian P. Gorman* [a2]

[a]Department of Materials Science and Engineering, University of North Texas,

Denton, 76203, USA

[b]VLSI Design and CAD Laboratory, University of North Texas, Denton, USA

[1]Department of Mathematics and Science, Brookhaven College,

Farmers Branch, TX 75244, USA

[2]Colorado Center for Advanced Ceramics, Department of Metallurgical and Materials

Engineering, Colorado School of Mines, Golden, CO 80401, USA.

Email-ID: umachoppali@gmail.com

Abstract

In this paper, synthesis of high quality nanocrystalline zinc oxide (ZnO) thin films is presented. A novel polymeric precursor route using ethylene diamine tetraacetic acid (EDTA) as chelating agent for Zn cations has been developed. The synthesized polymeric precursors were spincoated on different surface-modified substrates and were annealed at different temperatures. The effect of annealing, over the range of 300-600°C, on the properties of the ZnO films was investigated. The surface morphology, average crystallite size, degree of crystallization, and optical properties were also investigated. XRD results illustrate that the ZnO thin films are polycrystalline with texturing along the (002) plane. The thin films are dense, have homogeneous microstructure, with absorption edge at 375 nm, and optical transparency of over 85% in the visible region. The optical band gap energy of ZnO films was found to red-shift on annealing. Room temperature photoluminescence spectra of these films show strong UV emission on annealing.

Key words: ZnO, thin films, nanocrystalline, polymeric precursor, EDTA

1. Introduction

Zinc oxide (ZnO) is an n-type direct wide band-gap semiconductor (3.3eV) with large exciton binding energy of 60 meV at room temperature with near UV-emission. Owing to its optical properties, ZnO has plausible electro-optical applications, such as, solar cells [1, 2], light-emitting diodes [3, 4], UV lasers [5], thin film transistors [6,7], and UV photodetectors [8]. Besides these properties, ZnO thin films are chemically stable, non-toxic, bio-compatible, and are environmentally benign. ZnO thin films have been fabricated by various techniques, such as, pulsed laser deposition [9, 10], molecular beam epitaxy [11, 12], chemical vapor deposition [13], and sol–gel process [14-16].

However, thin film synthesis should be done via simple, cheap, convenient route for production at industrial scale, and easily adaptable for process control for reproducibility. The Pechini method [17] is one such processing technique that has been used for synthesis of several polycation oxides and perovskites [18- 20]. This process is an aqueous polymeric precursor route providing good stoichiometry, particle size control, and the added benefit of preparation in ambient atmosphere. In this process, an alpha-hydroxycarboxylic acid, such as citric acid, is generally employed as the chelating agent. However, it has been proven that ethylene diamine tetraacetic acid (EDTA) improves distribution of metal cations uniformly in the solution, resulting in high quality thin films. Research has been performed on synthesizing polymeric precursors using EDTA as chelating agent [21-22] for oxides.

To date, EDTA-derived ZnO thin films have not been prepared by the polymeric precursor method. In this paper, a novel simple modified aqueous polymeric precursor method is presented for synthesis of oxide thin films using EDTA as complexing agent. The modified precursor process has been implemented to synthesize smooth crack-free ZnO thin films on annealing. The paper further presents in-depth study of the effect of annealing on the properties of the ZnO thin films.

In this paper, nanocrystalline ZnO thin films prepared by a modified Pechini process have been studied in-depth. Citric acid in Pechini process has been replaced with EDTA as the complexing agent so as to increase the extent of chelation of Zn cations in the solutions. The prepared polymeric precursors were spincoated on surface modified substrates and annealed to different temperatures. Thermal evolution of the ZnO was studied by thermogravimetric analysis (TGA) and infra-red spectroscopy. Structural microstructure of the annealed thin films was characterized by XRD, SEM, and AFM. Room temperature photoluminescence (PL) and UV-transmission measurements were investigated to study the effect of annealing on optical properties of ZnO films.

2. Experimental Methods

2.1. Preparation of polymeric precursors and ZnO films

All chemicals acquired were of analytic-grade and were used as-received. ZnO polymeric precursors were prepared via the modified Pechini process using EDTA as the chelating agent. Zinc nitrate, $Zn(NO_3)_2.xH_2O$ (99%, Alfa Aesar), ethylene glycol (EG) (99%, Alfa Aesar), EDTA (99%, Acros), ammonium hydroxide, NH_4OH (29%, Fisher Scientific Inc.), and nitric acid, HNO_3 (70%, J. T. Baker) were used for preparing polymeric precursors. Deionized and filtered water (resistivity = 18.2MΩ) was used as the solvent in preparing the precursors.

A flow chart for the preparation of polymeric precursors using EDTA is shown in Fig.1. $Zn(NO_3)_2$, dissolved in deionized water, was standardized thermogravimetrically to calculate the amount of cation content. The amount of EDTA was determined by the molar ratio of EDTA to

Zn cations. 2.0 moles of EDTA were dissolved in 50ml of NH_4OH to facilitate its dissolution in deionized water. To this, 0.1 mole of zinc nitrate, dissolved in deionized and filtered water (resistivity = 18.2MΩ), was added to the solution, followed by 0.9 mole of EG. The resulting solution, with pH = 9, was then stirred and heated continuously at 80ºC. After heating for an hour, 0.1 mole of nitric acid was added drop-wise to the solution. Addition of nitric acid promotes polymerization, and hence, enhances the number of chelating sites for Zn cations. Although the pH decreased (pH = 7) on adding nitric acid, pH was maintained above 5 to prevent irreversible precipitation. The solution was heated constantly at 80ºC as temperatures less than 80ºC also resulted in a precipitated solution [22]. The solution was heated for approximately 10 hours while stirring continuously to obtain a clear, precipitate free solution with desired viscosity.

Glass microslides and silicon (2.54cm x 2.54cm) were used as substrates. The substrates were thoroughly rinsed ultrasonically in acetone, methanol, and deionized water. These were then immersed in 1N potassium hydroxide (KOH, EMD chemical Inc.) solution to modify the surface with hydroxyl ions so as to improve wetting characteristics of the substrates. The polymeric precursor was spincoated (CEE Model 100CB, Brewer Science, Inc., Rolla, MO) at 4000 rpm for 30s on the surface modified substrates, followed by curing at 70ºC on a hot plate for 1 hour for removal of residual water. The films were then annealed in air furnace at a ramp rate of 5ºC/min and were held for 10 minutes at temperatures of 300ºC, 450ºC, and 600ºC, respectively, for the pyrolization of the organic precursors and formation of ZnO.

2.2. Characterization of ZnO films

Thermogravimetric analysis (TGA, Perkin Elmer TGA-7) was used to monitor the pyrolysis of organic precursors and formation of the ZnO at a heating rate of 1°C/min under nitrogen atmosphere. Grazing incidence X-ray diffraction patterns were obtained on a Rigaku Ultima III X-ray diffractometer (Rigaku Corp., Tokyo, Japan) using CuKα radiation (40 kV and 44 mA) in the interval of 20° to 70°. The surface morphology of the annealed ZnO thin films was characterized by field emission scanning electron microscopy, FESEM, (Nova Nanolab 200, FEI Co.) and atomic force microscopy, AFM, (Multi-Mode Nanoscope IIIa, Digital Instruments). Annealed ZnO thin films were imaged in tapping mode of AFM using a silicon cantilever with a spring constant of 20–80 N/m at a scanning rate of 1 Hz. Surface roughness (root mean square, R_{rms}) was calculated using the software provided with the equipment. Thicknesses of the annealed films were determined by focused ion beam (FIB) cross-sections (Nova Nanolab 200, FEI Co., Hillsboro, OR). Changes in the optical transparency of the ZnO films in the visible region with annealing were monitored in transmission mode by a variable angle spectroscopic ellipsometer (VASE, J.A.Woollam Co. Inc., Lincoln, NE). The optical band-gap energy was estimated from optical transmittance and wavelength data, using an extrapolation of the linear portion of the plot of square of absorption coefficient (α^2) versus the photon energy ($h\nu$). Room temperature photoluminescence spectra were acquired using a scanning spectrofluorometer (Quantamaster QM-4, Photon Technology International) at an excitation wavelength of 320 nm using a Xenon lamp as an excitation source. The emission spectra were corrected for the detector response.

3. Results and discussion

Figure 2 shows the thermogravimetric analysis (TGA) curve of the synthesized polymeric precursors at a heating rate of 1ºC/min. The TGA analysis indicated a major weight loss (30%) between 30ºC and 150ºC, which corresponds to the evaporation of absorbed water and pyrolization of excess polyethylene glycol (PEG). A plateau is evident from 150ºC to 210ºC, indicating that the entire PEG has been pyrolized, leaving cross-linked network of EDTA and ethylene glycol with Zn cations in the film. This is followed by another weight loss (20%) between 210ºC and 255ºC. This loss may be due to pyrolization of EG. There is further weight loss (15%) up to 450ºC indicating that all of the organic precursors including EDTA have been removed [24], giving way to formation of ZnO. Beyond 450ºC, the weight decreases progressively upon further heating as the organics still present cannot be removed by oxidation in nitrogen atmosphere [25].

The ATR-FTIR absorption spectrum of the polymeric precursor prepared using EDTA and EG as chelating agents is shown in figure 3. A broad asymmetrical band between 2800 cm^{-1} and 3500 cm^{-1}, with few peaks of very weak intensities, is assigned to the presence of the O-H stretching mode of hydroxyl group and C-H stretching vibrations of the alkane groups. The peaks at 1320 cm^{-1}, 1390 cm^{-1}, 1420 cm^{-1} and 1590 cm^{-1} may be attributed to the bending modes of the O-H group [26, 27]. The strong, sharp bands at 1390 cm^{-1} and 1590 cm^{-1} may be attributed to the asymmetric and symmetric stretching modes of carboxylate group [22]. Bonding of metal cation to carbonyl group leads to sharp absorption peaks in the region of 1700 to 2200 cm^{-1} [26]. Absence of peaks within this spectral region illustrates that Zn cations are bonded to the hydroxyl group. The two strong bands appearing at 1040 cm^{-1} and 1080 cm^{-1} arise due to C-O stretching modes corresponding to the primary and secondary alcohols. The out-of-plane bending vibrations of C-H give rise to the band in the range of 850 cm^{-1} to 1000 cm^{-1}. The weak bands between 400 cm^{-1} and 850 cm^{-1} (fingerprint region) are the vibrations of the metal cations in the precursor [28]. FTIR spectra of the spincoated ZnO thin films (figure 4) illustrate the decomposition of the organic precursors and formation of the oxide with increase in annealing temperature. The characteristic bands of Zn-O vibrations appear at 444 and 457 cm^{-1} as shown in inset [29]. Additional peaks at 607 cm^{-1}, 669 cm^{-1}, and 1100 cm^{-1} arise due to silicon, which was used as substrate in these studies [30].

XRD spectra were acquired in the grazing incidence mode to determine the crystallite size, orientation, and average strain of annealed ZnO thin films deposited on silicon substrates. On annealing at 300ºC, diffraction peaks related to ZnO are not observed in the XRD spectrum, as shown in Fig. 5a. This observation reconfirms TGA data indicating the presence of organic precursors and absence of ZnO at 300ºC. The XRD spectrum of 450ºC-annealed ZnO thin films exhibit diffraction peaks which can be indexed to polycrystalline wurtzite ZnO (space group $P6_3mc$; JCPDS no. 36-1451, Fig. 5b). One of these peaks at $2\theta = 51.3^\circ$ is not a ZnO diffraction peak and may be related to carbon. Presence of this peak suggests that the organic precursors are not completely pyrolyzed at 450ºC. On annealing at 600ºC (Fig. 5c), the diffraction peak at $2\theta = 51.3^\circ$ disappears revealing that the thin films synthesized are of pure ZnO. On annealing, the intensity of the peaks increased due to improved crystallinity. The full width at half maximum (FWHM) of the (002) diffraction peak of the ZnO thin films decreases from 0.51º to 0.43º on annealing from 450ºC to 600ºC suggesting grain growth at high temperatures. The crystallite size was estimated using Scherrer's method and was found to be 28.5 nm and 33.7 nm for 450ºC and 600ºC, respectively. Moreover, there is no shift in the diffraction peak positions as compared to bulk ZnO indicating that the thin films are strain free even when annealed at high temperatures.

It is also observed that there is texturing in the ZnO films along the (002) plane on annealing above 450ºC.

SEM micrographs of annealed ZnO thin films prepared by spin-coating using EDTA-derived polymeric precursors are displayed in Fig. 6. Samples annealed at 300ºC show smooth, highly porous structure due to the presence of organic precursors (Fig. 6a) confirming that ZnO does not form at 300ºC. Mean surface roughness (R_{rms}) of these films, as determined by AFM, was found to be 2.592 nm. Micrographs of ZnO thin films annealed at 450ºC (Fig. 6b) illustrate uniformly distributed homogeneous granular structure with an average grain size of 60 – 70 nm and surface roughness of 14.07 nm. On annealing at 600ºC (Fig. 6c), ZnO films are dense, mono-dispersed, homogeneous with spherical morphology, and without cracks. The average grain size and surface roughness of these films decreased to 25 – 30 nm and 3.59 nm, respectively. This decrease in average grain size contradicts the fact that there is always grain growth on annealing. Presence of unpyrolized organic matter at 450°C may be the cause of an increase in average grain size and increased roughness of the films. On annealing at 600°C, there is complete pyrolysis and formation of pure ZnO.

The thickness of ZnO thin films annealed at 450ºC and 600ºC was obtained from FIB cross-sections. Films annealed at 450ºC and 600ºC were about 25 nm and 130 nm thick, respectively. The cross-section of 600ºC film on silicon substrate appears dense with texturing, as shown in Fig. 7.

Fig. 8 shows spectral dependencies of transmission in the wavelength range 260 - 750 nm for the annealed ZnO thin films. The film annealed at 300ºC (Fig. 8a) does not show absorption edge for the whole range suggesting that formation of ZnO did not take place. ZnO films annealed at 450ºC and 600ºC (Fig. 8b and 8c) exhibit an average transmittance of above 85% in the visible region suggesting superior optical quality. The transmission increases sharply in the visible region due to onset of fundamental absorption of ZnO. It is observed that on annealing, there is a decrease in transmission in the visible region attributed to an increase in optical scattering due to rough surface [31-33]. There is a shift in absorption edge with annealing attributed to grain growth.

The optical absorption coefficient, α was evaluated from transmission spectra by the following: $\alpha = {}^{1}/_{\mathrm{d}} \ln \mathrm{T}$ where d is the thickness of the film obtained from FIB cross-sections and T is the transmittance. The absorption coefficient, α varies with photon energy, $h\nu$, by following the relationship:

$$\alpha = \frac{C(h\nu - E_g)^{\frac{1}{2}}}{h\nu} \qquad (1)$$

where C is a constant and E_g is the optical band gap for allowed direct band transition. Figure 9 shows the Tauc plot of $(\alpha h\nu)^2$ versus photon energy, $h\nu$ of the annealed ZnO films. Linear dependence of $(\alpha h\nu)^2$ versus $h\nu$ at higher energy indicates that the annealed ZnO films are direct band semiconductors. The optical band gap values were determined by extrapolating the linear portion of the Tauc plots to intersect the energy axis. The optical band gap of the films decreased from 3.298 eV to 3.194 eV on annealing from 450ºC to 600ºC. This band gap narrowing is due to improved crystallinity and grain growth usually observed in direct band transition semiconductors [32].

Room temperature PL emission spectra of annealed ZnO thin films in the range of 350 – 550 nm for different annealing temperatures are shown in Fig. 10. The emission spectra were collected using a Xenon lamp under photon excitation of 320 nm. ZnO film annealed at 300ºC did not show any UV emission due to absence of ZnO and hence, reconfirming the XRD and

SEM data. PL spectra of 450ºC and 600ºC-annealed films show near UV emission peak attributed to free - exciton recombination near band edge [31, 34]. No peak was observed in the visible region, which is attributed to the presence of structural defects. There is no significant change in intensity of near UV emission peak on annealing. The UV emission peak has considerably red - shifted on annealing from 380.4nm at 450ºC to 384.7nm at 600ºC.

The refractive index, n and the extinction coefficient, k of the annealed ZnO films were calculated from the transmittance data [35]. Figure 11 shows the variation of refractive index with wavelength in the range of 380 – 800 nm. The refractive index decreased with increase in wavelength in the visible region. Moreover, the refractive index increased from 1.67 to 1.93 at 380 nm on annealing from 450ºC to 600ºC which is slightly lower than n = 2 for bulk ZnO. The extinction coefficient, k, is related to the absorption coefficient, α, by $k = \alpha\lambda/4\pi$ where λ is the wavelength. Change in the extinction coefficient with wavelength is shown on Fig. 12. It is observed that the extinction coefficient decreased with rise in annealing temperatures suggesting improved stoichiometry of the ZnO films. For 450ºC-annealed films, there is a steep decline in the extinction coefficient near the absorption edge as compared to the 600ºC-annealed films.

The refractive index depends on the relative density of the thin films. The relative density was calculated using the Lorentz-Lorenz equation for ZnO films [36, 37]:

$$\text{Relative density (\%)} = \frac{(n^2-1)(n_b^2+2)}{(n_b^2-1)(n^2+2)} \text{ x } 100\% \qquad (2)$$

where n and n_b are the refractive indices of the film and the bulk ZnO (2.0), respectively [38]. The relative densities of the annealed ZnO thin films increased on annealing; from 75% at 450ºC to 95% at 600ºC at 385 nm. The densities of the annealed ZnO films also decreased with increase in wavelength.

ZnO thin films have been fabricated via modified polymeric precursor process using EDTA and EG as chelating agents. EDTA is chosen as chelating agent to study its strong chelating power to chelate Zn cations. It is observed that the molar ratios of the reactants determine the microstructure of ceramic films synthesized via polymeric precursor process [37]. When the ratio of EDTA/EG was greater than 2, the spincoated films appeared continuous but they cracked on annealing. Since the spincoated films have to be pyrolysed, the amount of organics has to be minimized to prevent cracking in the films [21]. For a lower ratio, there is a possibility that the Zn cations may not get chelated. Therefore, the ratio of EDTA/ EG was chosen to be around 2 as it produced continuous, dense, crack-free ZnO thin films.

EDTA has been chosen as complexing agent as it provides six chelating bonds. ZnO thin films have been synthesized using other complexing agents such as citric acid, glycerol, and EG [20, 37, 39]. It is found that ZnO films have hexagonal flower-like morphology instead of continuous thin films when derived from EG-based polymeric precursors [39]. Glycerol and citric acid derived ZnO thin films have a smooth microstructure but EDTA-derived ZnO films have smaller crystallite sizes comparable to glycerol and citric acid complexing agents. The advantage of using EDTA in place of citric acid or glycerol is that it provides better chelating power and the grain size is small even when annealed at 600ºC. These films are better suited for high temperature applications as the effect of sintering on grain growth is quite slow.

4. Conclusions

High quality nanocrystalline ZnO thin films have been synthesized by a novel modified polymeric precursor method using EDTA as chelating agent. ZnO thin films have not been synthesized by this modified method until now. Results show that ZnO is formed when annealed at temperatures higher than 300°C. Polycrystalline wurtzite ZnO thin films are formed, which is supported by TGA, XRD, and SEM data. The ZnO films are smooth, stress free, without cracks, dense, and have 85% transmittance in the visible region. The effect of annealing on these ZnO films was also studied. TGA and XRD results indicate that all organics get pyrolysed only on annealing at 600°C. ZnO thin films, annealed at 600°C, show texturing along the (002) plane with increase in annealing temperature. SEM micrographs reveal that the grain size decreases with increase in annealing temperatures, which is due to the presence of unpyrolized organic matter. Transmittance spectra illustrate that the annealed ZnO films are highly transparent in the visible region and have a band edge at about 375 nm. There is a decrease in optical band gap energy with increase in annealing temperature due to grain growth. The films exhibit strong PL emission in the near UV region suggesting high quality of the films.

Acknowledgement

The authors thank Dr. Richard Reidy and his group for their assistance in transmission measurements. They also thank Dr. Mohammed Omary and his group of Department of Chemistry, University of North Texas, for their assistance in photoluminescence measurements.

References

[1] Y. Lare, A. Godoy, L. Cattin, K. Jondo, T. Abachi, F.R. Diaz, M. Morsli, K. Napo, M.A. del Valle, J.C. Bernède, ZnO thin films fabricated by chemical bath deposition, used as buffer layer in organic solar cells, Appl. Surf. Sci 255 (2009) 6615-6619.

[2] Z.A. Wang, J.B. Chu, H.B. Zhu, Z. Sun, Y.W. Chen, S.M. Huang, Growth of ZnO:Al films by RF sputtering at room temperature for solar cell applications, Solid State Electron. 53 (2009) 1149-1153.

[3] H. Kim, J.S. Horwitz, W.H. Kim, A.J. Mäkinen, Z.H. Kafafi, D.B. Chrisey, Doped ZnO thin films as anode materials for organic light-emitting diodes, Thin Solid Films 420 – 421 (2002) 539-543.

[4] H. Ohta, K. Kawamura, M. Orita, M. Hirano, N. Sarukura, H. Hosono, Current injection emission from a transparent p –n junction composed of p-$SrCu_2O_2$ /n-ZnO, Appl. Phys. Lett. 77 (2000) 475 - 477.

[5] M. H. Huang, S. Mao, H. Feick, H. Yan, Y.Wu, H. Kind, E.Webber, R. Russo and P. Yang, Room-Temperature Ultraviolet Nanowire Nanolasers, Science 292 (2001) 1897-1899.

[6] W. I. Park, G. C. Yia, J.-W. Kim, S.M. Park, Schottky nanocontacts on ZnO nanorod arrays, Appl. Phys. Lett., 82 (2003) 4358 - 4360.

[7] Dhananjay, S. B. Krupanidhi, Low threshold voltage ZnO thin film transistor with a $Zn_{0.7}Mg_{0.3}O$ gate dielectric for transparent electronics, J. Appl. Phys. 101 (2007) 123717.

[8] U. Özgür, Ya. I. Alivov, C. Liu, A. Teke, M. A. Reshchikov, S. Dogan, V. Avrutin, S. J. Cho, and H. Morkoc, A Comprehensive Review of ZnO Materials and Devices, J. Appl. Phys., 98 (2005) 041301.

[9] T. Nakamura, H. Minoura, H. Muto, Fabrication of ZnO(0001) epitaxial films on the cubic(111) substrate with C_6 symmetry by pulsed laser ablation, Thin Solid Films 405 (2002) 109 - 116.

[10] A. Klini, A. Manousaki, D. Anglos, C. Fotakis, Growth of ZnO thin films by ultraviolet pulsed-laser ablation: Study of plume dynamics, J. Appl. Phys. 98 (2005) 123301.

[11] Y. W. Heo, D. P. Norton, S. J. Pearton, Origin of green luminescence in ZnO thin film grown by molecular-beam epitaxy, J. Appl. Phys. 98 (2005) 073502.

[12] X. Yang, J. Zhang, Z. Bi, Y. He, Q. Xu, H. Wang, W. Zhang, X. Hou, Glancing-incidence X-ray analysis of ZnO thin films and ZnO/ZnMgO heterostructures grown by laser-MBE, J. Cryst. Growth 284 (2005) 123 - 128.

[13] M. Purica, E. Budianu, E. Rusu, M. Danila, R. Gavrila, Optical and structural investigation of ZnO thin films prepared by chemical vapor deposition (CVD), Thin Solid Films 403–404 (2002) 485- 488.

[14] C.-Y. Tsay, K.-S. Fan, S.-H. Chen, C.-H. Tsai, Preparation and characterization of ZnO transparent semiconductor thin films by sol–gel method, J. Alloys Compd. 495 (2010) 126.

[15] J. Petersen, C.Brimont, M.Gallart, O.Crégut, G.Schmerber, P.Gilliot, B.Hönerlage, C. Ulhaq-Bouillet, J.L.Rehspringer, C.Leuvrey, S.Colis, A.Slaoui, A.Dinia, Optical properties of ZnO thin films prepared by sol–gel process, Microelectron. J. 40 (2009) 239–241.

[16] J. Zhang, H. Feng, W. Hao, T. Wang, Blue-emitting ZnO sol and film obtained by sol-gel process, J. Sol-Gel Sci. Technol. 39 (2006) 37 - 39.

[17] M.P. Pechini, US Patent No. 3,330,697, July 1967.

[18] Q. N. Pham, M. Vijayakumar, C. Bohnke, O. Bohnke, Synthesis and electrical characterization of $Li_{0.30}Ca_{0.35}TaO_3$ perovskite synthesized via a polymerized complex route, J. Solid State Chem. 178 (2005) 1915 - 1924.

[19] R. K. Gupta, C. M. Whang, Effects of anion and synthesis route on the structure of $(La_{0.9}Sr_{0.1})(Cr_{0.85}Fe_{0.05}Co_{0.05}Ni_{0.05})O_{3-\delta}$ perovskite and removal of impurity phases, Solid State Ionics 178 (2007) 1617 - 1626.

[20] U. Choppali, B. P. Gorman, Structural and optical properties of nanocrystalline ZnO thin films synthesized by the citrate precursor route, J. Lumin. 128 (2008) 1641-1648.

[21] V. Agarwal, M. Liu, Preparation of barium cerate-based thin films using a modified Pechini process, J. Mater. Sc. 32 (1997) 619 - 625.

[22] D. Zhou, G. Huang, X. Chen, J. Xua, S. Gong, Synthesis of $LaAlO_3$ via ethylenediaminetetraacetic acid precursor, Mater. Chem. Phys. 84 (2004) 33 -36.

[24] Y. E. Zhao, C. Y. Cai, Y. Y. Luo, Z. H. He, FTIR Spectra of the $M(EDTA)^{n}-$ Complexes in the Process of Sol-Gel Technique, J. Supercond. 17 (2004) 383 - 387.

[25] D. Mondelaers, Chemical Solution Deposition of ZnO Thin Films by an Aqueous Solution Gel Precursor Route, J. Sol-Gel Sci. Technol. 26 (2003) 523 - 526.

[26] B.M. Keyes, L.M. Gedvilas, X. Li, T.J. Coutts, Infrared spectroscopy of polycrystalline ZnO and ZnO:N thin films, J. Cryst. Growth 281 (2005) 297 - 302.

[27] G. Socrates, Infrared and Raman Characteristic Group Frequencies. Wiley, New York, 2001.

[28] Y.-J. Lin, Y.-H. Chang, W.-D. Yang, B.-S. Tsai, Synthesis and characterization of ilmenite NiTiO3 and CoTiO3 prepared by a modified Pechini method, J. Non-Cryst. Solids 352 (2006) 789 - 794.

[29] P. R. Patil, S. S. Joshi, Polymerized organic–inorganic synthesis of nanocrystalline zinc oxide, Mater. Chem. Phys. 105 (2007) 354 - 361.

[30] O. M. Ntwaeaborwa, P. H. Holloway, Enhanced photolumine^{3+}scence of Ce induced by an energy transfer from ZnO nanoparticles encapsulated in SiO2, Nanotechnology 16 (2005) 865 - 868.

[31] P. Sagar, P.K. Shishodia, R.M. Mehra, H. Okada, A. Wakahara, A. Yoshida, Photoluminescence and absorption in sol–gel-derived ZnO films, J. Lumin. 126 (2007) 800 - 806.

[32] M. Wang, E. J. Kim, J. S. Chung, E.W. Shin, S. H. Hahn, K. E. Lee, C. Park, Influence of annealing temperature on the structural and optical properties of sol–gel prepared ZnO thin films, Phys. Stat. Sol. (a) 203 (2006) 2418 – 2425.

[33] C.-Y. Tsay, H.-C. Cheng, Y.-T. Tung, W.-H. Tuan, C.-K. Lin, Effect of Sn-doped on microstructural and optical properties of ZnO thin films deposited by sol–gel method, Thin Solid Films 517 (2008) 1032 - 1036.

[34] L. Wischmeier, T. Voss, S. Borner, W. Schade, Comparison of the optical properties of as-grown ensembles and single ZnO nanowires, Appl. Phys. A 84 (2006) 111 – 116.

[35] J. C. Manifacier, J. Gasiot, J. P. Fillard, A simple method for the determination of the optical constants *n*, *k* and the thickness of a weakly absorbing thin film, J. Phys. E. 9 (1976) 1002 - 1004.

[36] S. Bandyopadhyay, G. K. Paul, S. K. Sen, Study of optical properties of some sol–gel derived films of ZnO, Sol. Energy Mater. Sol. Cells. 71 (2002) 103 - 113.

[37] U. Choppali, B. P. Gorman, Nanocrystalline ZnO Thin Film Synthesis Using Glycerol in Aqueous Polymeric Precursor Processing, J. Am. Ceram. Soc., 91 (2008) 2553 - 2558.

[38] M. Ohyama, H. Kozuka, T. Yoko, Sol-gel preparation of ZnO films with extremely preferred orientation along (002) plane from zinc acetate solution, Thin Solid Films 306 (1997) 78 – 85.

[39] U. Choppali, B. P. Gorman, Controlling the Morphology of Polymeric Precursor-Derived ZnO Flower-Like Structures, J. Am. Ceram. Soc. 90 (2007) 433 - 442.

Figure Captions

Figure 1: Flow-chart of procedure for the preparation of EDTA-derived polymeric precursor and the ZnO thin films.

Figure 2: TGA curve (heating rate = 2ºC/min) of ZnO polymeric precursor prepared using ethylene glycol and EDTA as chelating agents.

Figure 3: ATR spectra of polymeric precursor prepared using EDTA and ethylene glycol as chelating agents.

Figure 4: FTIR spectra of annealed ZnO thin films synthesized from polymeric precursor, prepared using EDTA and ethylene glycol as chelating agents. Inset shows the vibrations characteristic to ZnO at different annealing temperatures.

Figure 5: XRD spectra of polymeric precursor based ZnO thin films annealed at: (a) 300°C, (b) 450°C, and (c) 600°C.

Figure 6: SEM micrographs of the ZnO thin films synthesized using EDTA based polymeric precursor and annealed at: (a) 300°C, (b) 450°C, and (c) 600°C.

Figure 7: Micrograph of FIB cross-section of ZnO thin films on silicon substrate annealed at 600°C. The image shows that the ZnO films are 130nm thick and textured.

Figure 8: Optical transmittance spectra of EDTA-derived ZnO thin films annealed at (a) 300°C, (b) 450°C, and (c) 600°C.

Figure 9: Tauc plots of annealed polymeric precursor derived ZnO thin films. The band gap decreased from 3.316 eV to 3.194 eV with increase in annealing temperature from 450°C to 600°C.

Figure 10: Room temperature photoluminescence of ZnO thin films prepared from EDTA polymeric precursors and annealed at (a) 300°C, (b) 450°C, and (b) 600°C.

Figure 11: Variation of refractive index of EDTA-derived ZnO thin films with increase in annealing temperature.

Figure 12: Extinction coefficient of EDTA-derived annealed ZnO thin films as a function of wavelength.

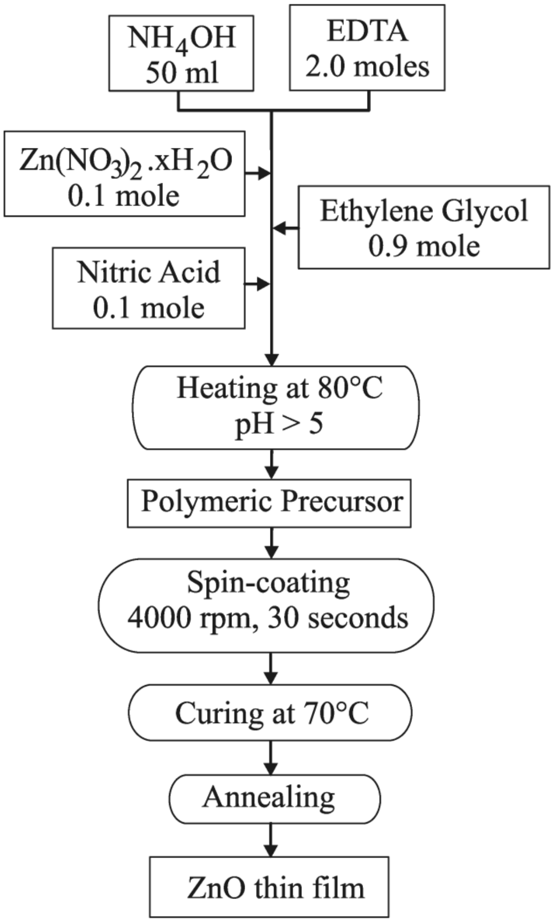

Fig. 1: Flow-chart of procedure for the preparation of EDTA-derived polymeric precursor and the ZnO thin films.

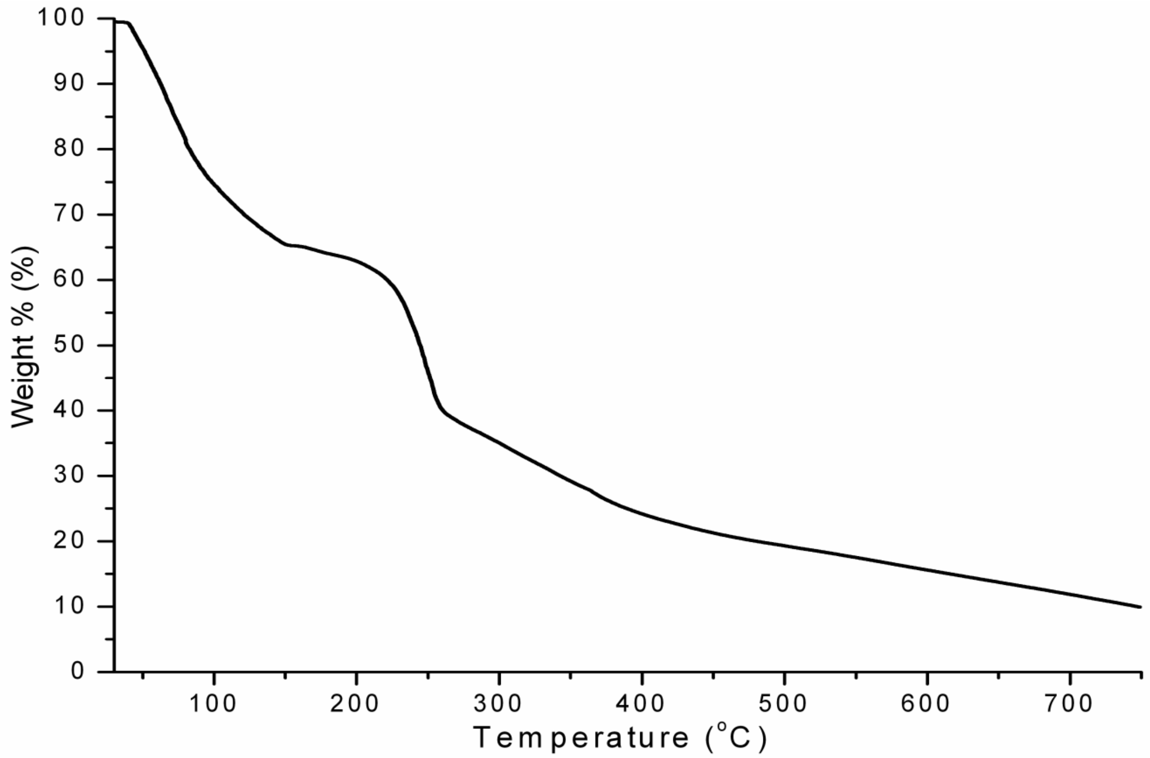

Fig. 2: TGA curve (heating rate = 2ºC/min) of ZnO polymeric precursor prepared using ethylene glycol and EDTA as chelating agents.

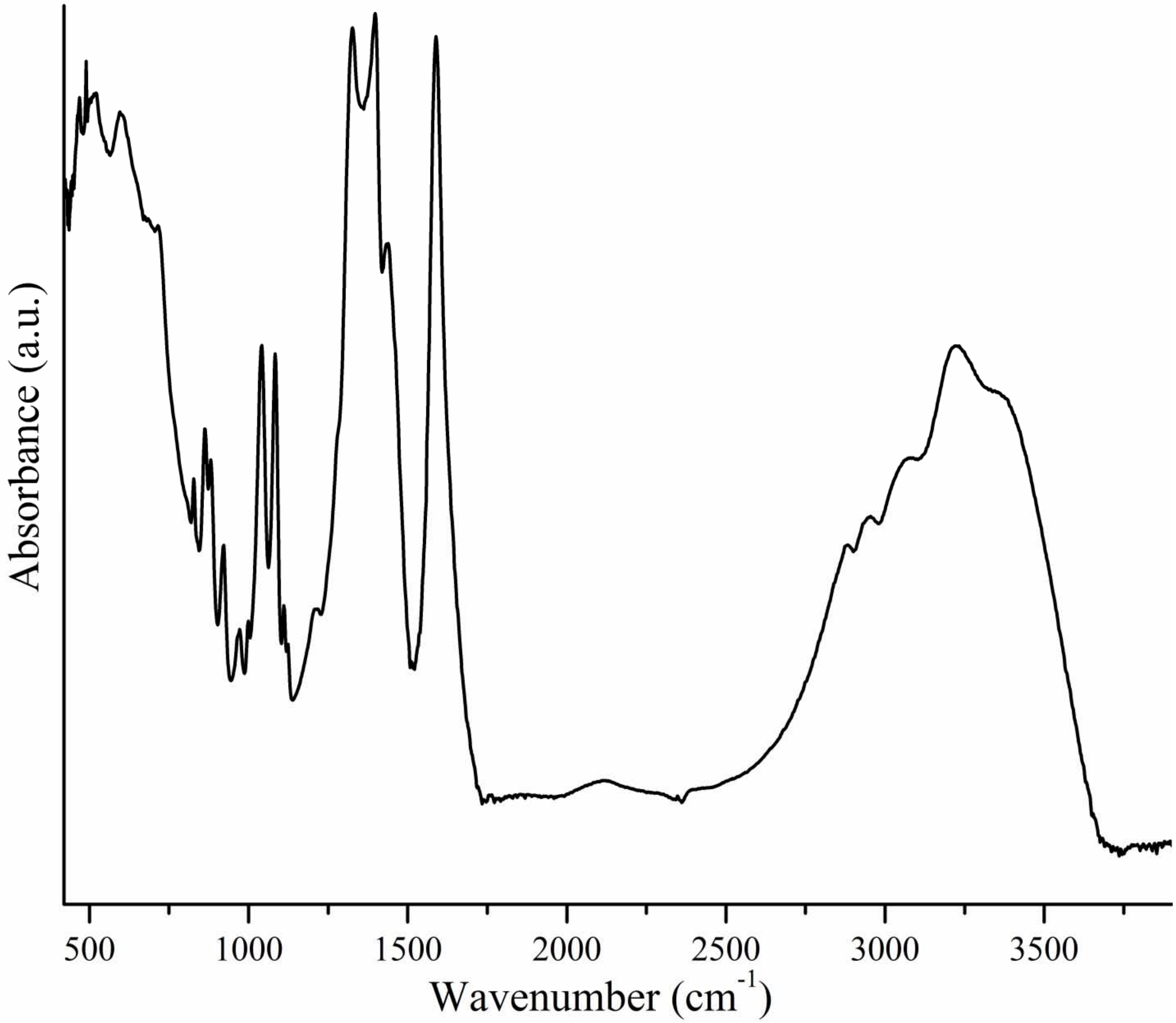

Fig. 3: ATR spectra of polymeric precursor prepared using EDTA and ethylene glycol as chelating agents.

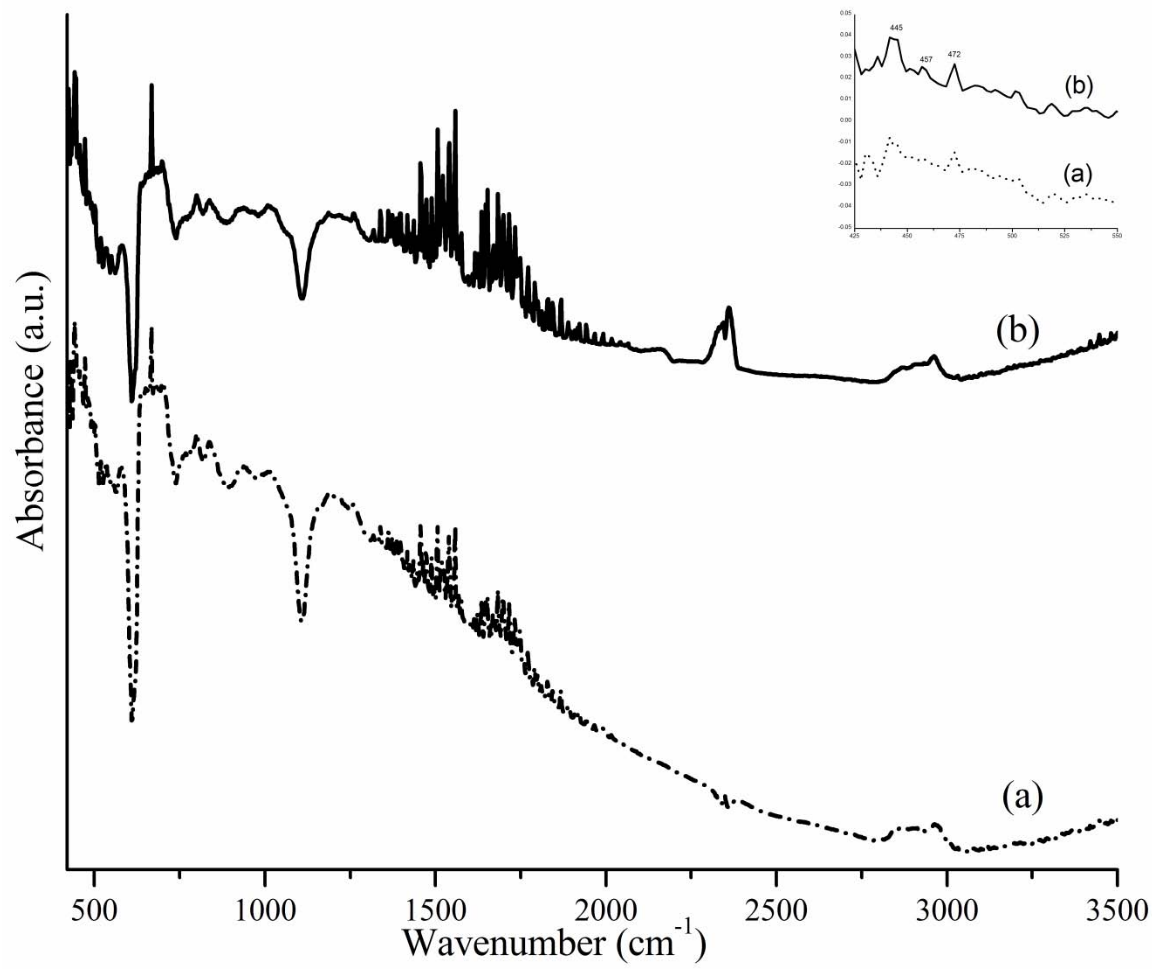

Fig. 4: FTIR spectra of annealed ZnO thin films synthesized from polymeric precursor, prepared using EDTA and ethylene glycol as chelating agents. Inset shows the vibrations characteristic to ZnO at different annealing temperatures.

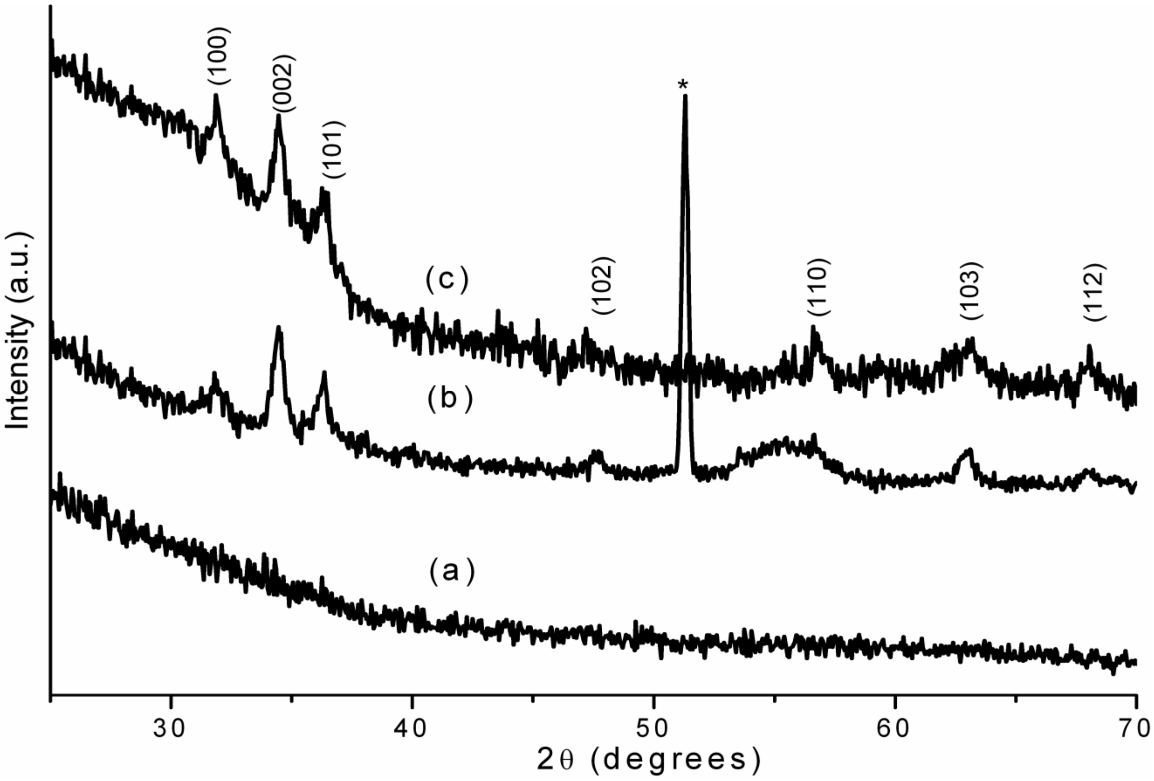

Fig. 5: XRD spectra of polymeric precursor based ZnO thin films annealed at: (a) 300°C, (b) 450°C, and (c) 600°C.

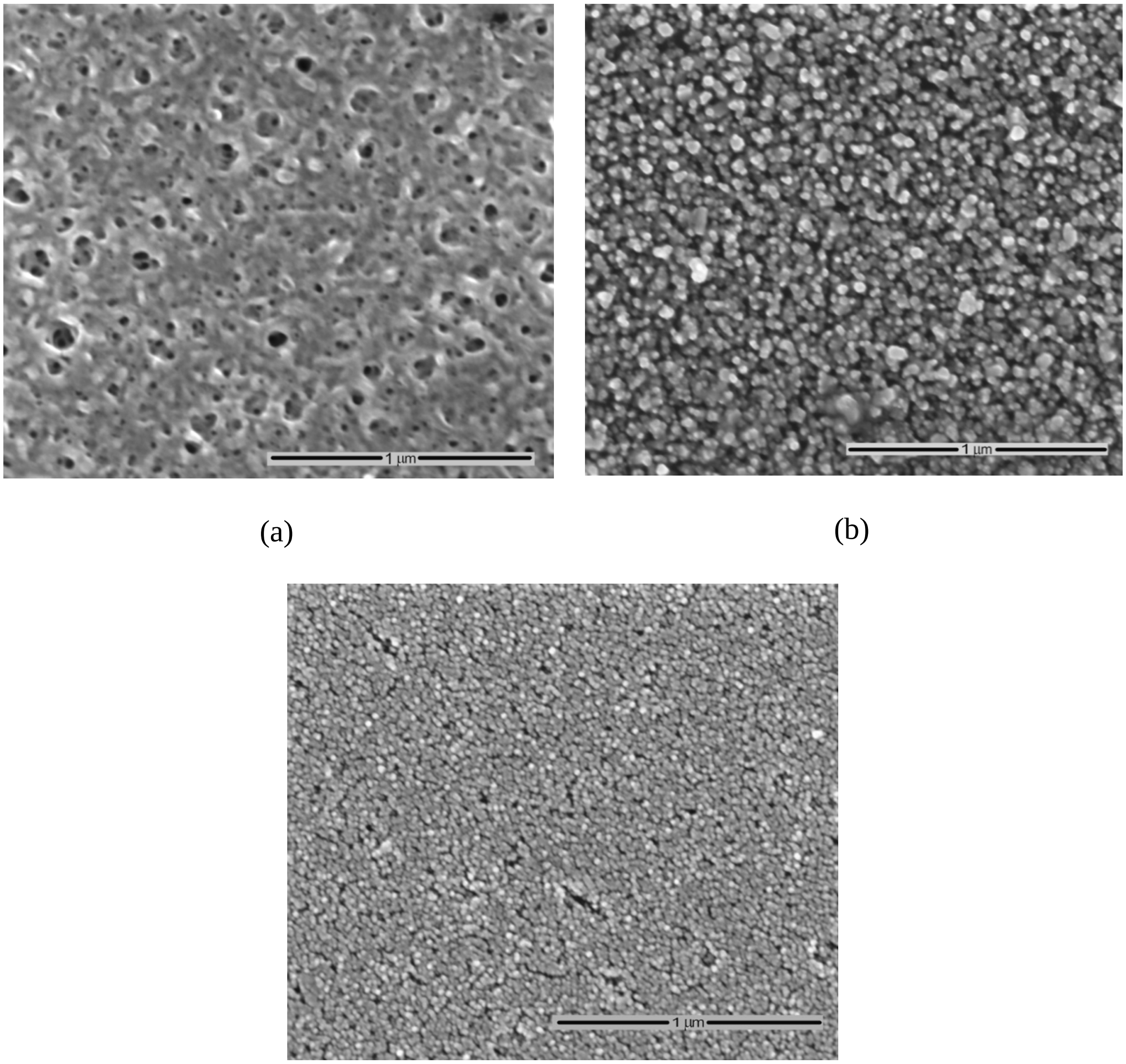

(a)

(b)

(c)

Fig. 6: SEM micrographs of the ZnO thin films synthesized using EDTA based polymeric precursor and annealed at: (a) 300°C, (b) 450°C, and (c) 600°C.

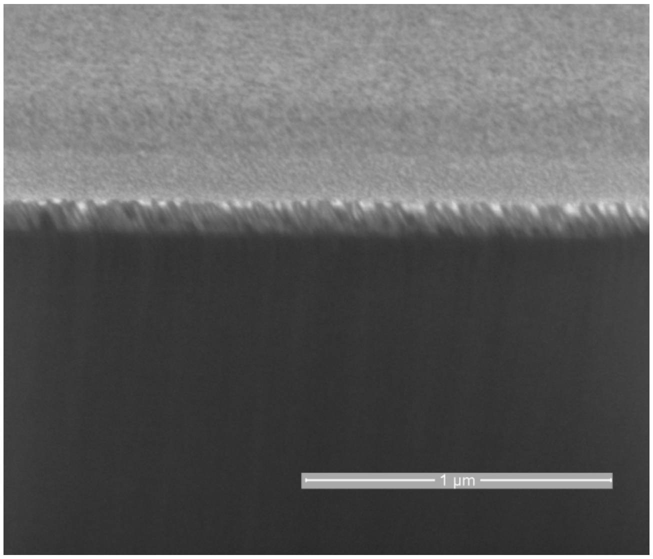

Fig. 7: Micrograph of FIB cross-section of ZnO thin films on silicon substrate annealed at 600°C. The image shows that the ZnO films are 130nm thick and textured.

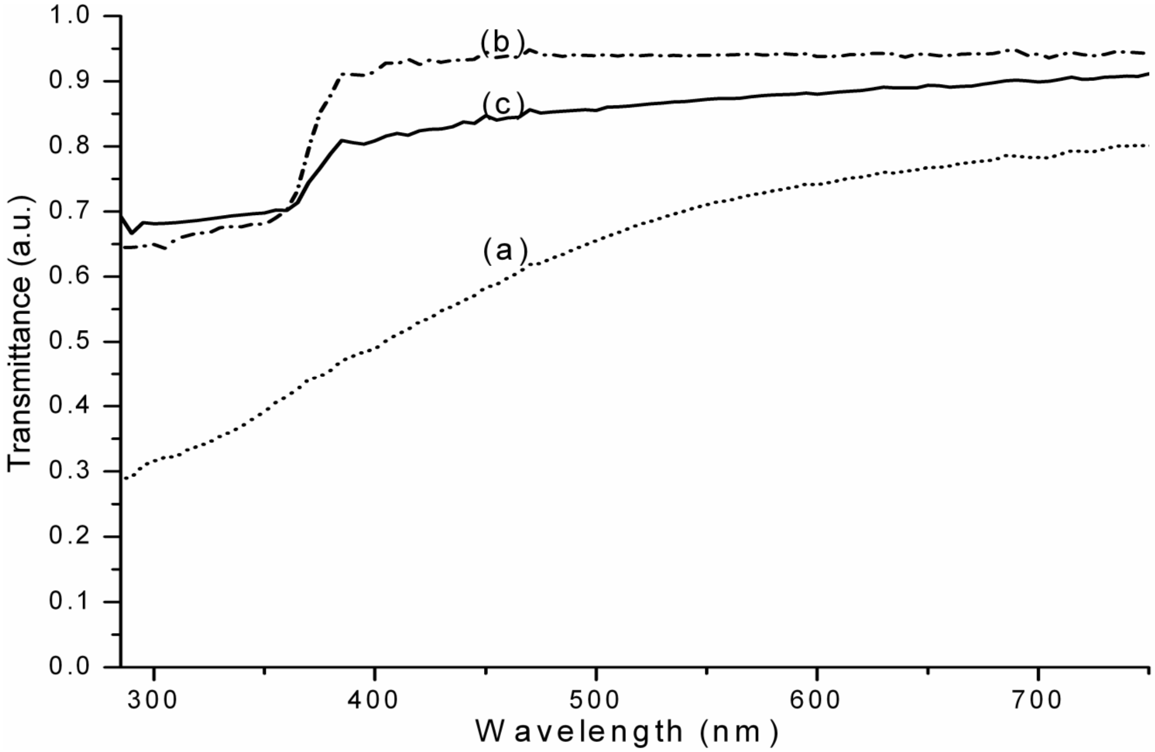

Fig. 8: Optical transmittance spectra of EDTA-derived ZnO thin films annealed at (a) 300°C, (b) 450°C, and (c) 600°C.

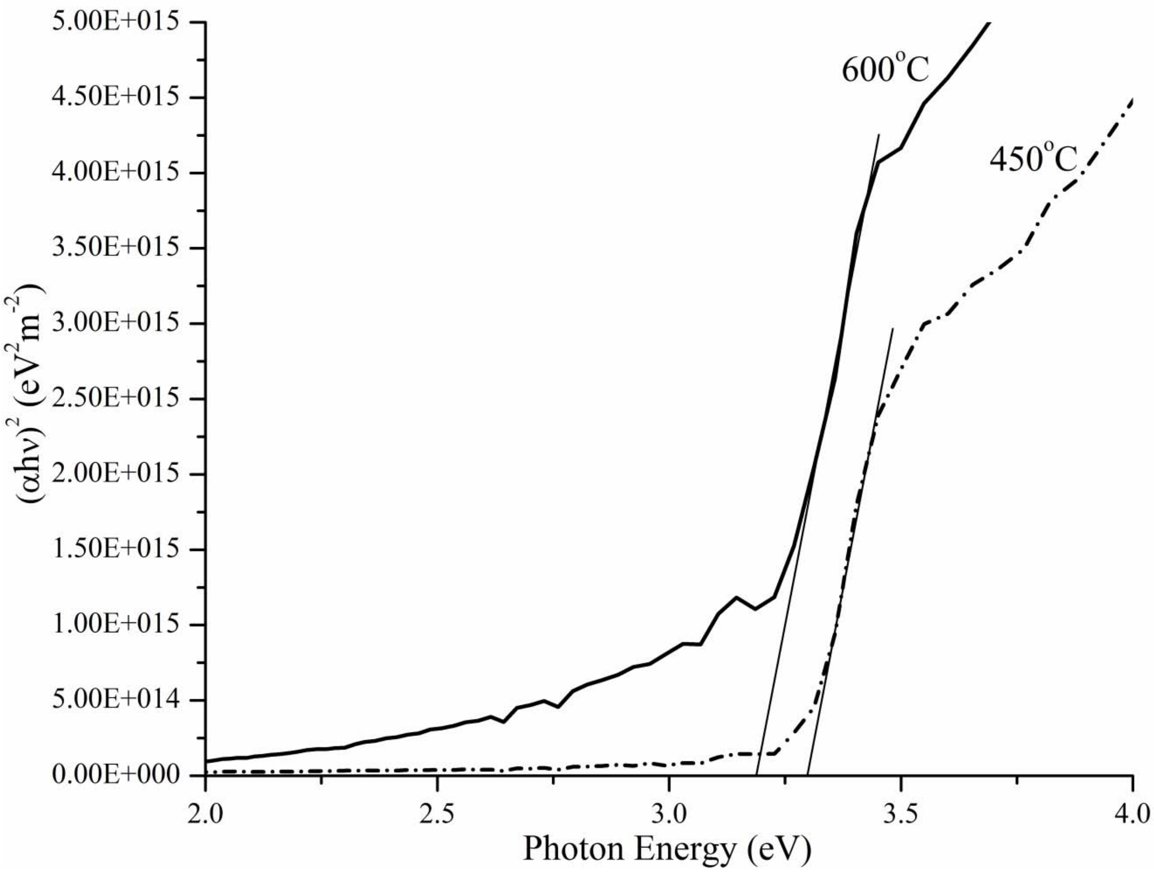

Fig. 9: Tauc plots of annealed polymeric precursor derived ZnO thin films. The band gap decreased from 3.298 eV to 3.194 eV with increase in annealing temperature from 450°C to 600°C.

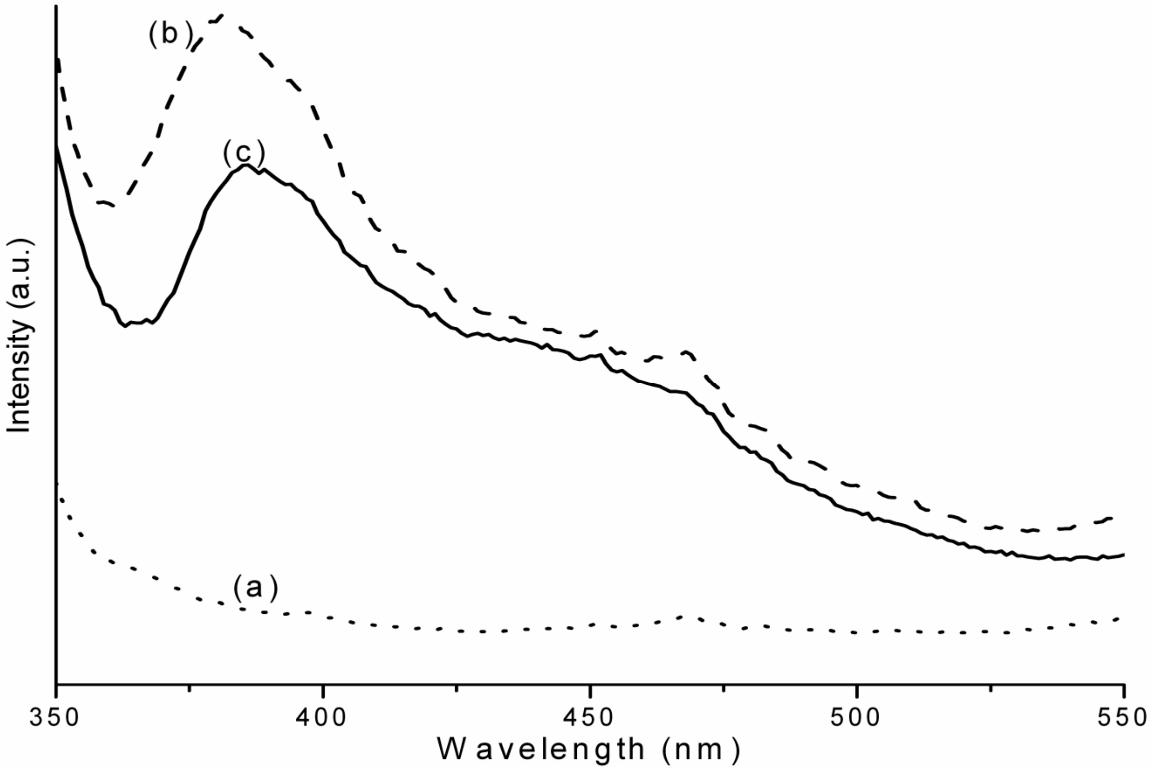

Fig. 10: Room temperature photoluminescence of ZnO thin films prepared from EDTA polymeric precursors and annealed at (a) 300°C, (b) 450°C, and (b) 600°C.

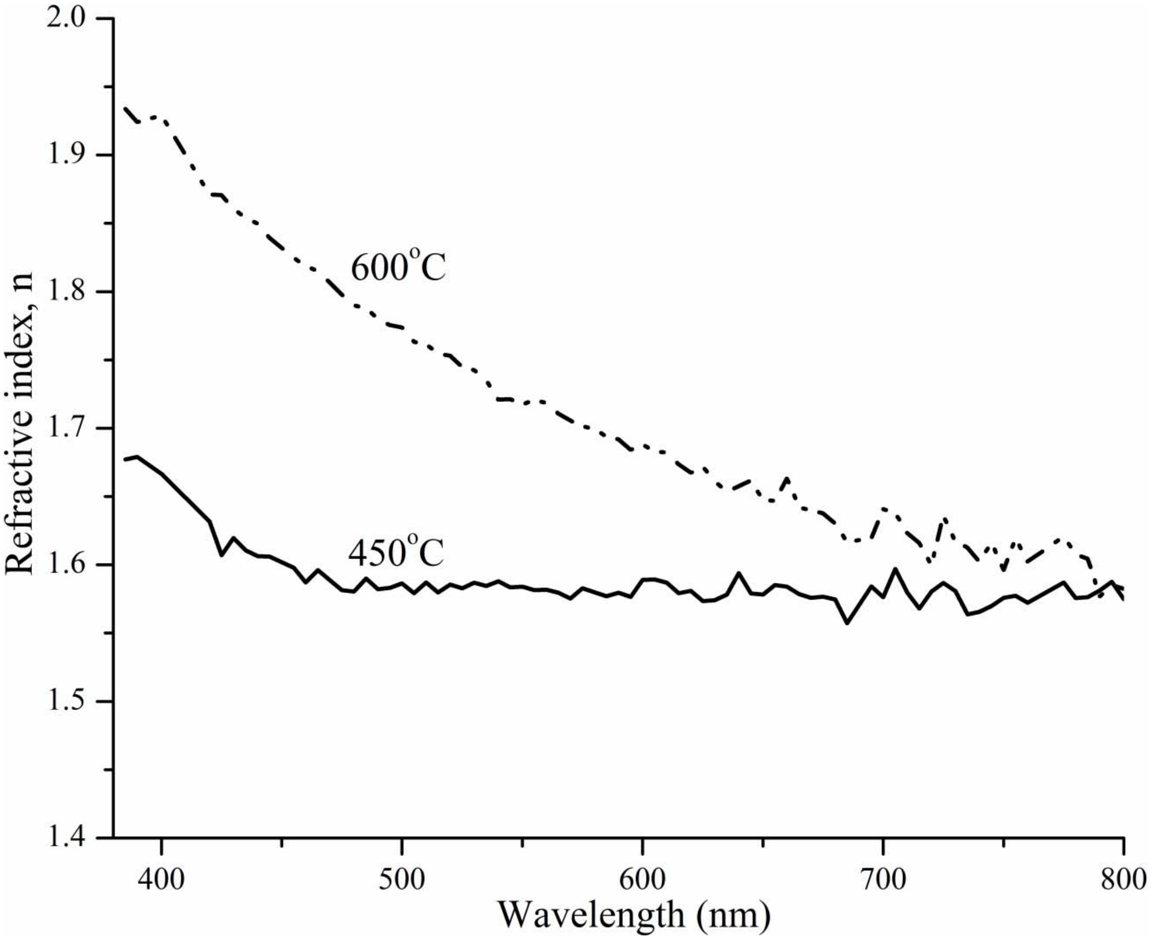

Fig. 11: Variation of refractive index of EDTA-derived ZnO thin films with increase in annealing temperature.

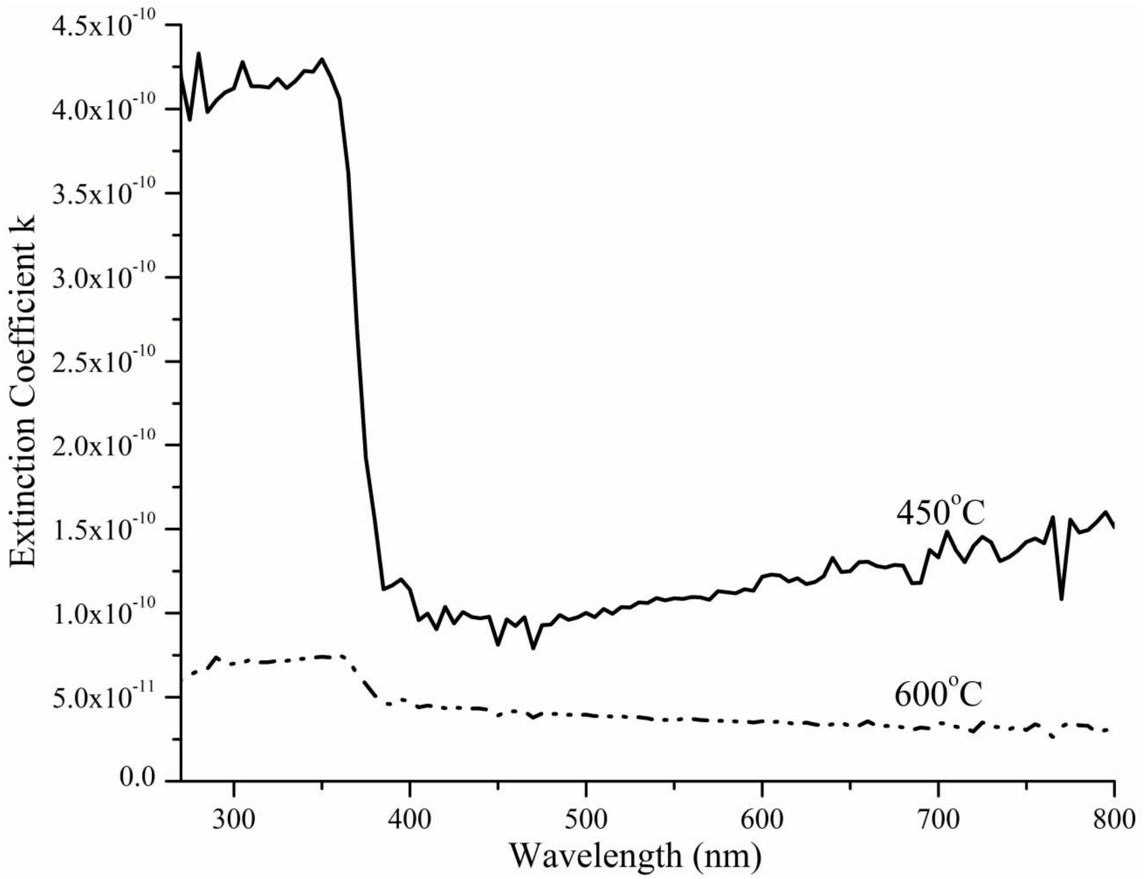

Fig. 12: Extinction coefficient of EDTA-derived annealed ZnO thin films as a function of wavelength.